BUILD SIMUL
https://doi.org/10.1007/s12273-019-0583-8

Gene-expression programming for the assessment of surface mean pressure coefficient on building surfaces

Monalisa Mallick[1] (✉), Abinash Mohanta[2], Awadhesh Kumar[1], Kanhu Charan Patra[1]

1. Department of Civil Engineering, National Institute of Technology Rourkela, Rourkela, Odisha, 769008, India
2. Department of Mechanical Engineering, Vellore Institute of Technology, Vellore, Tamilnadu, 632014, India

Abstract

Wind surface mean pressure coefficient ($\bar{C}_p$) is an essential parameter for the assessment of wind induced forces that is a must input to all structural designs. An extensive experimentation is carried out to obtain pressure coefficient data over the surfaces of C-shaped building models of varying aspect ratio, corner curvature and angle of incidence in a sub-sonic wind tunnel. The studies also include models without corner curvature. In this study, a technique known as Gene-Expression Programming (GEP) is used to develop a model equation using experimental values of pressure coefficient data collected at the grid points of the frontal surface under varying conditions. And this developed model is used to predict surface mean pressure coefficients ($\bar{C}_p$). The predicted values of $\bar{C}_p$ using the developed model are compared with the corresponding $\bar{C}_p$ values obtained by Swami and Chandra (S&C) equation and Muehleisen and Patrizi (M&P) equations. The prediction made by the developed GEP model is also validated with the actual building data of Tokyo Polytechnic University (TPU). The results signify the ability of the model to predict the $\bar{C}_p$ values for practical purposes. The error analysis of the results show that the predicted values of $\bar{C}_p$ using developed GEP correlation are more close to the experimental values than those obtained by using other two methods.

Keywords

C-shaped building models,
wind tunnel test,
surface mean pressure coefficient,
gene-expression programming,
error analysis

Article History

Received: 26 February 2019
Revised: 30 July 2019
Accepted: 17 September 2019

© Tsinghua University Press and Springer-Verlag GmbH Germany, part of Springer Nature 2020

1 Introduction

Increased usage of a range of new innovative building design requires an accurate assessment of the wind-induced pressure and its impact on the structures. Accurate assessment/prediction of wind pressure or pressure coefficient will lead to a safer structure. Wind pressure on the structures is affected by the geometry of the structure, the nature of the corner (with or curvature), incidence angle of wind and flow features. Generally, experiments are conducted on small-scale models in a wind tunnel to collect pressure coefficient data on grid points marked on the surfaces of the model. The pressure coefficient data thus collected is used for the analysis and development of the generalized model equations. These predicted values of pressure coefficients are used in the design of a prototype structure.

Cook (1990) reported on wind pressures on irregular shapes. Ho et al. (1990) examined the interference of local obstructions on low building wind loads. Stathopoulos and Zhou (Stathopoulos and Zhou 1993; Zhou and Stathopoulos 1997) studied the wind loads on the stepped-roof of L-shape building by the numerical approach. A considerable investigation has been reported on different structures, i.e., cylindrical, rectangular and square (Macdonald 1975; Meroney 1988; Lin et al. 2005). The literature shows only few studies for irregular building models. Ahmad and Kumar (2001) tested a model of a hip roof building (30° roof slope) at Texas Tech University (TTU) on a scale ratio of 1:50 in the simulated wind. They compared the pressure values data obtained from the model test with the real pressure data of the prototype. Lou et al. (2005) carried out wind tunnel tests on a double-skin facade building to find out the wind pressure distribution on each surface. Gomes et al. (2005) investigated pressure distributions on L- and U-shaped building models under varying wind incidence angle. Suresh Kumar et al. (2006) estimated C_p values on the faces of a

E-mail: monalisa.nitrkl@gmail.com

tall building from the experiment conducted on the model in a wind tunnel. Lu et al. (2007) carried out a numerical simulation of pressure distribution on the surface of a spherical tall building with and without subsidiary curved annexes. Amin and Ahuja (2008, 2011) presented their works on L- and T-shaped buildings for different configurations and estimated the average, minimum, maximum and root mean square values of pressure coefficients. Chakraborty et al. (2013) reported the pressure distribution of a '+' (plus) shaped tall building and compared by numerical analysis using Fluent. Kim and Kanda (2013) studied the fluctuating values of wind pressures, flow separation and formation of the vortex on tall buildings as well as conical shaped building. Bhattacharyya et al. (2014) reported on the pressure distribution of E-shaped tall buildings under a varying angle of incidences from 0° to 180°. Chakraborty et al. (2014) carried out a comparative study between the experimental and the numerically obtained values of pressure coefficient to predict wind effect on '+' plan shaped tall building. Yi and Li (2015) conducted an experiment on a model of a tall building at Hong Kong in a wind tunnel to explain wind force and pressure coefficients at high frequency balance technique. The wind tunnel test result was seen to be fairly equivalent with the full model test. Li and Li (2016) also conducted a wind tunnel experiment on L plan shaped tall building to quantify dynamic load on the building. They proposed an empirical formulation to assess wind load. Bhattacharyya and Dalui (2018) investigated mean wind pressures on E plan shaped tall building and compared between the experimental and the numerical results by CFD.

Akins (1976), Walton (1982), and Walker and Wilson (1993) proposed parametric equations for the prediction of C_p on low rise buildings. Ginger and Letchford (1999) and Ohkuma et al. (1991) studied the pressure coefficients on a particular building (full-scale) tests. Grosso (1992) proposed a complex parametric model equation for pressure coefficient on the surfaces of the buildings. Swami and Chandra (1987) presented surface-average pressure coefficients on the facades of the low rise buildings. Swami and Chandra (1988) proposed an equation for the prediction of C_p at different levels of rectangular shaped buildings considering the wind direction and side ratio. This equation is used to forecast the surface average pressure coefficient (C_p) which is widely implemented by Crawley et al. (2001) for generating a program named as Building Energy Simulation. Cook (2007) proposed a code using analytical wind load calculation techniques to estimate the average wind pressure coefficients for the buildings of common shapes. Cóstola et al. (2009, 2010) presented a review of many equations and methodologies of calculating C_p and included airflow network analysis in building energy simulations. Further, Muehleisen and Patrizi (2013) developed an equation for the prediction of C_p values for the cases of low rise buildings.

Recently, the machine learning algorithms (MLAs) are used extensively as the alternative approach for predicting the flow properties in areas of aerodynamics. Bre et al. (2018) proposed artificial neural network (ANN) models to predict the surface averaged pressure coefficients for each wall and roof according to the building geometry and the wind angles. Recently, the gene-expression programming (GEP) has drawn a lot of attentions over the other soft computing techniques in engineering fields as its added advantage for its capability of generating simplified equation without assuming a preceding form of the existing relationship (Cousin and Savic 1997; Drecourt 1999; Savic et al. 1999; Whigham and Crapper 1999, 2001; Babovic and Keijzer 2002; Karimi et al. 2016). GEP also has a unique, multigenic nature which consents the development of more complex programs composed into several subprograms. Limited studies exist in the literature, in the use of GEP to the engineering field (Harris et al. 2003; Giustolisi 2004; Guven and Gunal 2008; Guven and Aytek 2009; Azamathulla et al. 2013; Pradhan and Khatua 2018). Das et al. (2019) applied the GEP technique to develop a model for predicting discharge in non-prismatic diverging and converging type compound channels and showed that GEP performed better as compared to the DCM. Karimi et al. (2016) proposed a new combination method for predicting short-term and long-term stream flows by using wavelet gene-expression programming. Wang et al. (2016) investigated the capabilities of gene-expression programming models to calculate ET0 using meteorological variables in China and compare the ability of GEP and ANN techniques. The ability of the GEP used to estimate daily dew point temperature at two stations in the northwest of Iran and concluded that in the temperature-based scenarios, T_{min} is the most effective parameter (Mehdizadeh et al. 2017).

There are many reports in literature related to the regular plan shape of buildings and a few reports for irregular plan shape of buildings. The detailed studies on the surfaces of such irregular shape of buildings are important for the current trends of the building. From the literature reviews, it is seen that the wind induced pressure coefficient on the surfaces of irregular plan shape of buildings such as L, T, E, +, Y, and U etc. mainly depends upon the building geometry, angle of incidence and surroundings. The literature provides limited works for L, T, E, +, Y and U shaped buildings but does not provide any information on C-shaped building plans. For U-shaped buildings, only single curvature has been used in the studies. In practice, many large hotels, museums, academic and other public buildings are in use C-shaped buildings. Fysikern building (Red C-shaped building) in Upper Lappis, (Northern Djurgarden, Sweden), Robert C.

Weaver Federal Building (Washington, D.C., USA), C-Shaped Wright House in Durban (South Africa) and Ring of Celestial Bliss (Taiwan, China) are some examples of applicability of such structures. Therefore, in the present research work, the curvature effects have been studies in detail by taking models of four different curvatures. The extensive experimentation has been carried out to obtain mean pressure coefficient with varying corner curvature in addition to varying aspect ratio, side ratio and angle of incidence.

The present study is focussed on finding out a reliable method for predicting the surface mean pressure coefficient ($\overline{C}_p$) at the frontal surface of C-shaped building models. Gene-expression programming (GEP) is used for developing the equation to predict the $\overline{C}_p$ value. In this current study, the authors considered the four influencing parameters such as curvature ratio (R/D), side ratio with curvature (D/B) or side ratio without curvature (d/b), height ratio (D/H), and angle of incidence (θ) are used as inputs to the model for predicting the output ($\overline{C}_p$). Estimation of the surface mean pressure coefficient for other traditional methods (S&C and M&P model) is also computed and respective performance analysis is carried out to measure the effectiveness of the proposed model.

2 Experimental setup

2.1 Features of experimental setup

Experiments are carried out in an open circuit sub-sonic wind tunnel in the Aerodynamics Laboratory of the Department of Aerospace Engineering, Indian Institute of Technology Kharagpur (IITK), India. The wind speed is kept constant at 12.9 m/s. The wind tunnel with a bottom surface made up of plywood a test section is 1.83 m long and cross-sectional dimensions of 0.61 m × 0.61 m. Building models are placed within the boundary layer zone, centrally in the test section at a distance of 1.2 m from the beginning of the test section. To ascertain models within the boundary layer zone, the roughness elements are placed on the upstream side of the model. For this, wooden cubic blocks of 25 mm size and clear spacing of 50 mm in all directions are fixed on 4 mm thick plywood sheet. Photocopy of Sub-Sonic wind tunnel with schematic illustration is shown in Fig. 1. The velocity profile inside the wind tunnel has a power-law index (n) of 0.143. The velocity profile within the wind tunnel test section and the turbulence intensity are shown in Figs. 2(a) & (b) respectively.

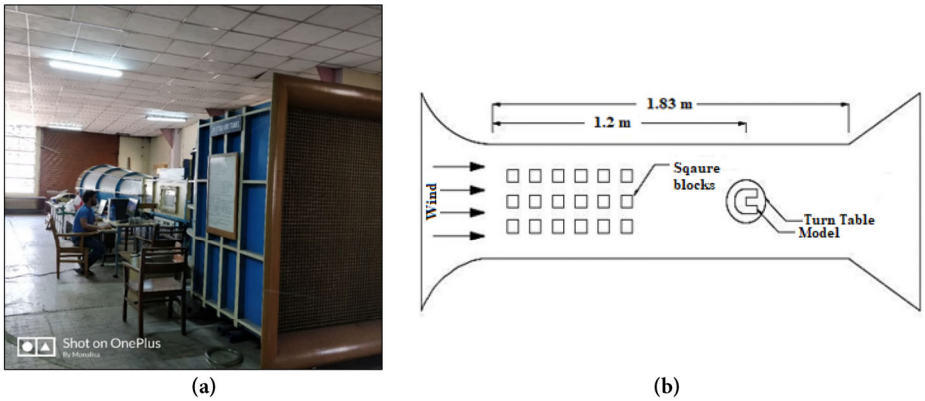

Fig. 1 (a) The photocopy of sub-sonic wind tunnel (IIT Kharagpur, India); (b) schematic diagram for experimental setup of wind tunnel

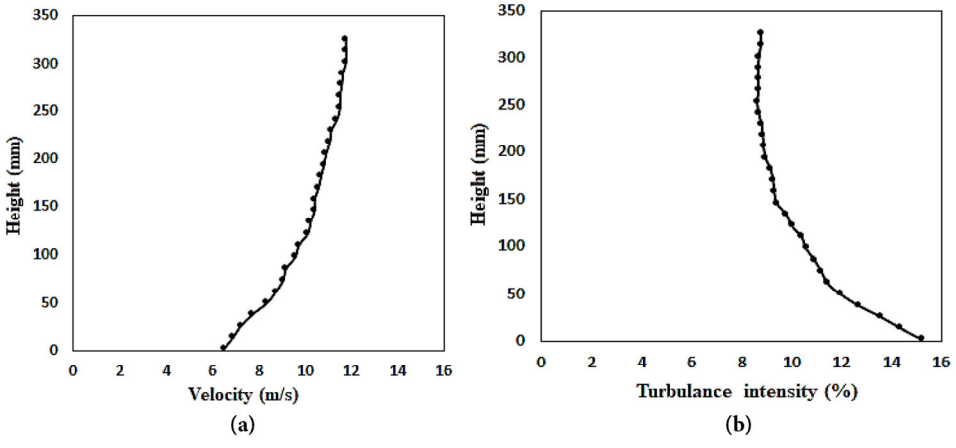

Fig. 2 Variation of: (a) velocity profile at the test section; and (b) turbulence intensity with height at test section

2.2 Model design

All the experimental building models are made of transparent Perspex sheet of 3 mm thickness. Geometrical configuration of a C-shaped building model is shown in Fig. 3. Surface 1 is the face perpendicular to wind flow known as a frontal face, and surface 2 is the side face of the model. The C-shaped building model consists of overall width (B), width without curvature (b), overall depth (D), depth without curvature (d), radius of curvature (R) and height (H) as shown in Fig. 3(a). Thirteen C-shaped models having corner curvature are tested by varying curvature ratios (C-1, C-2, C-3 and C-4), frontal ratios (C-5, C-6 and C-7), side ratios (C-8, C-9, and C-10) and height ratios (C-11, C-12 and C-13). In C-14, C-15, and C-16 building models, overall width (B) is equal to width without curvature (b), and overall depth (D) is equal to depth without curvature (d) as there is no corner curvature ($R = 0$) as shown in Fig. 3(b). Three models without corner curvature (C-14, C-15, and C-16) by varying side ratios with constant height ratios are also used for the wind tunnel test. Figures 4(a) and (b) present a photocopy of the actual model with and without corner curvature of C-shaped building model. Details of the model configurations are given in Table 1.

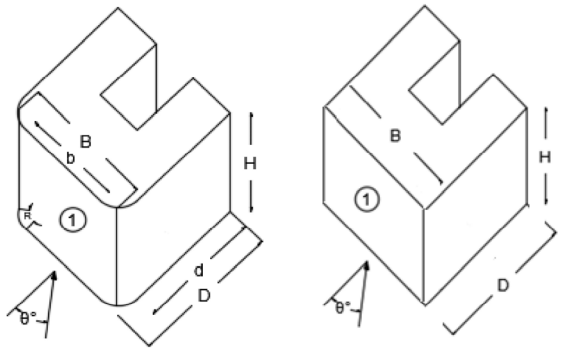

(a) (b)

Fig. 3 Geometry of building models defining the surfaces, dimensions, and angle of incidence: (a) C-shaped model with curvature; and (b) C-shaped model without curvature

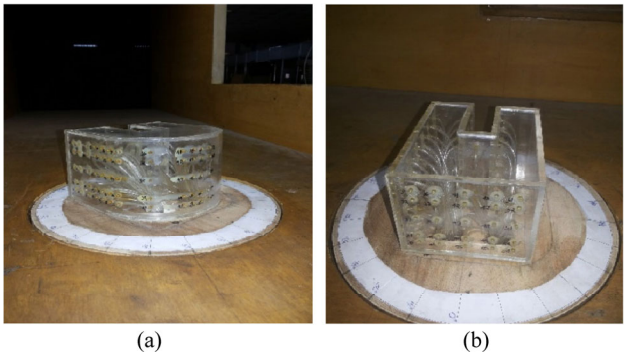

(a) (b)

Fig. 4 Photograph of experimental building models: (a) C-shaped model with curvature; and (b) C-shaped model without curvature

Table 1 Geometry of different c-shaped building models used in the experimental process

Sl. No.	Models name	Overall depth D (mm)	Overall width B (mm)	Depth d (mm)	Width b (mm)	Height H (mm)	Radius of curvature R (mm)
1	C-1	120	120	100	80	80	20
2	C-2	120	120	90	60	80	30
3	C-3	120	120	80	50	80	40
4	C-4	120	120	70	40	80	50
5	C-5	110	120	80	60	80	30
6	C-6	100	120	70	60	80	30
7	C-7	90	120	60	60	80	30
8	C-8	120	110	90	50	80	30
9	C-9	120	100	90	40	80	30
10	C-10	120	90	90	30	80	30
11	C-11	120	120	90	60	70	30
12	C-12	120	120	90	60	60	30
13	C-13	120	120	90	60	50	30
14	C-14	120	120	120	120	80	0
15	C-15	120	90	120	90	80	0
16	C-16	100	75	100	75	80	0

2.3 Process of experimentation

Free stream velocity during the experiment is measured with the help of the Pitot tube. The models are fitted with 90 to 120 numbers of pressure tapping points in 4–5 rows and 3–5 columns on the surfaces. The pressure tapping points are kept at less spacing near the wall boundaries to tap the sharp pressure variation due to flow separation and at a larger spacing in the middle of the surfaces. The free ends of tubes are connected to Digital Sensor Array (DSA) to record the fluctuating wind pressure at the corresponding tapping points. All data are measured by a DSA scan valve corporation, model DSA 3217/16 pox, USA. This DSA device is set to give an average pressure of 5 s duration. At the same time, for greater accuracy, a pressure measurement at each tapping point is repeated for three times and the mean of three pressure data is obtained. The pressure coefficient (C_p) for each tapping point is calculated by putting the pressure data in Eq. (1) given as:

$$C_p = \frac{P - P_\infty}{P_0 - P_\infty} \tag{1}$$

where P = mean pressure data obtained experimentally, P_∞ = static pressure in the reference tube and P_0 = total pressure in the settling chamber.

Surface mean wind pressure coefficients of C-shaped building models are calculated using the pressure coefficient

data obtained experimentally over the surface. The pressure coefficient data are recorded under varying depth to breadth (D/B) ratios as 1, 0.92, 0.83, 0.75, 1.09, 1.2, and 1.33, depth to height (D/H) ratios as 1.5, 1.71, 2, and 2.24 and wind angles as 0° to 180° at 15° intervals. The wind angle θ is measured with respect to the perpendicular drawn on the frontal surface 1 as shown in Fig. 3. The model is fixed on a turn table which is placed at the middle of the test section of the wind tunnel. With the help of turn table, the model is rotated up to 180° in counter clockwise direction for measuring surface pressure on the marked grid points at an interval of 15°. At zero angle of incidence, the front face of the model is placed perpendicular to the wind flow direction. At this position of the model, the pressure coefficient is calculated for each taping point using the unstable wind pressure record. From these pressure coefficient data, surface mean pressure coefficient is obtained. This same procedure is repeated for the surfaces of all the models of varying configurations. The values of surface mean pressure coefficients data as obtained for the models of varying curvatures are given in Table 2. Table 3 presents the surface mean pressure coefficient values for the surfaces of the models without curvature.

3 Development of model for predicting $\bar{C}_p$

Modeling is a process of creating, testing and validating a process with some probability to forecast the outcomes. The model involves two types of parameters, i.e., dependent and independent. After the collection of data from relevant parameters, some statistical tools, and analytical techniques are used to develop the model. Researchers have tried purpose analytical based models to predict the surface mean pressure coefficient $\bar{C}_p$. Previously, Swami and Chandra (1988) proposed an equation for calculating the mean pressure coefficient at surfaces of low-rise building and is termed as S&C equation, given as:

$$\begin{aligned}\bar{C}_p(\theta, D/B) = \bar{C}_p(0^\circ)\ln[1.248 - 0.703\sin(\theta/2) \\ - 1.175\sin^2(\theta) + 0.131\sin^3(2G\theta) \\ + 0.769\cos(\theta/2)! + 0.07G^2\sin^2(\theta/2) \\ + 0.717\cos^2(\theta/2)]\end{aligned} \quad (2)$$

where, θ indicates the angle of wind incidence on the surface, G the logarithmic of the ratio side face described as $\ln(D/B)$ and $\bar{C}_p$ (0°) the $\bar{C}_p$ value at 0° angle of incidence. Further, Muehleisen and Patrizi (2013) developed the model for the

Table 2 Surface mean pressure coefficient ($\bar{C}_p$) on surface 1 of different building models with varying corner curvatures

Model name	Model parameters				Value of $\bar{C}_p$												
	D/B	d/b	D/H	R/D	0°	15°	30°	45°	60°	75°	90°	105°	120°	135°	150°	165°	180°
C-1	1.00	1.25	1.50	0.17	0.70	0.66	0.48	0.22	−0.16	−0.42	−0.81	−0.89	−0.72	−0.68	−0.53	−0.50	−0.50
C-2	1.00	1.50	1.50	0.25	0.80	0.68	0.41	0.03	−0.36	−0.75	−0.84	−0.91	−0.76	−0.72	−0.62	−0.53	−0.49
C-3	1.00	2.00	1.50	0.33	0.80	0.74	0.50	0.31	−0.19	−0.55	−0.85	−0.90	−0.77	−0.69	−0.63	−0.52	−0.48
C-4	1.00	3.50	1.50	0.42	0.84	0.75	0.43	−0.15	−0.52	−0.79	−0.89	−0.94	−0.91	−0.85	−0.74	−0.61	−0.56
C-5	1.00	1.50	1.71	0.25	0.74	0.68	0.53	0.22	−0.17	−0.56	−0.81	−0.90	−0.84	−0.76	−0.59	−0.51	−0.46
C-6	1.00	1.50	2.00	0.25	0.71	0.69	0.51	0.21	−0.22	−0.53	−0.74	−0.79	−0.59	−0.51	−0.49	−0.43	−0.41
C-7	1.00	1.50	2.40	0.25	0.72	0.70	0.59	0.32	−0.15	−0.48	−0.63	−0.68	−0.55	−0.36	−0.28	−0.25	−0.23
C-8	0.92	1.33	1.50	0.27	0.76	0.68	0.55	0.31	−0.14	−0.57	−0.77	−0.88	−0.66	−0.56	−0.53	−0.49	−0.45
C-9	0.83	1.17	1.50	0.30	0.75	0.70	0.51	0.27	−0.09	−0.41	−0.63	−0.77	−0.68	−0.50	−0.40	−0.35	−0.33
C-10	0.75	1.00	1.50	0.33	0.75	0.72	0.57	0.22	−0.16	−0.43	−0.50	−0.48	−0.43	−0.40	−0.36	−0.31	−0.30
C-11	1.09	1.80	1.50	0.25	0.69	0.68	0.54	0.24	−0.28	−0.63	−0.90	−0.97	−0.76	−0.62	−0.51	−0.41	−0.37
C-12	1.20	2.25	1.50	0.25	0.81	0.78	0.61	0.12	−0.32	−0.61	−0.85	−0.91	−0.77	−0.61	−0.52	−0.45	−0.42
C-13	1.33	3.00	1.50	0.25	0.77	0.71	0.54	0.13	−0.36	−0.67	−0.90	−0.92	−0.80	−0.66	−0.54	−0.41	−0.36

Table 3 Surface mean pressure coefficient ($\bar{C}_p$) on surface 1 of different building models without corner curvatures

Model name	Model parameters		Value of $\bar{C}_p$												
	D/B	D/H	0°	15°	30°	45°	60°	75°	90°	105°	120°	135°	150°	165°	180°
C-14	1.00	1.50	0.79	0.78	0.65	0.41	0.04	−0.37	−0.62	−0.70	−0.56	−0.49	−0.40	−0.40	−0.36
C-15	1.33	1.50	0.74	0.70	0.64	0.34	−0.09	−0.60	−0.77	−0.72	−0.62	−0.57	−0.50	−0.42	−0.37
C-16	1.33	1.50	0.79	0.74	0.63	0.32	−0.17	−0.55	−0.78	−0.71	−0.60	−0.56	−0.50	−0.46	−0.43

mean pressure coefficient at a wall of a low-rise building by a various angle of incidence, θ and the side ratio D/B and is termed as (M&P) equation given as:

$$\bar{C}_p(\theta, D/B) = \frac{a_0 + a_1 G + a_2\theta + a_3\theta^2 + a_4 G\theta}{1 + b_1 G + b_2\theta + b_3\theta^2 + b_4 G\theta} \quad (3)$$
$$G = \ln(D/B)$$

where, a_i and b_i are the adjustable factors with different values described below, θ the angle of incidence, and G the logarithmic of the ratio side face described as ln(D/B). The values of a_i and b_i are given as:

$a_0 = 6.12\times10^{-1}$, $a_1 = -1.78\times10^{-1}$, $a_2 = -1.15\times10^{-2}$,
$a_3 = 3.28\times10^{-5}$, $a_4 = 1.67\times10^{-3}$, $b_1 = -3.12\times10^{-1}$,
$b_2 = -1.59\times10^{-2}$, $b_3 = 9.82\times10^{-5}$, $b_4 = 2.15\times10^{-3}$

3.1 New model approach

In this present work, a data driven technique is applied to predict the surface mean pressure coefficient ($\bar{C}_p$). The most popular database method from the data driven field is the gene-expression programming (GEP) which is adopted here to obtain a model for the prediction of $\bar{C}_p$ on the surface of C-shaped models having with curvature ratios ranging from 0.17 to 0.42 (Table 2) and without curvature model is zero curvature having side ratio from 1.00 to 1.33 (Table 3). In this study, GeneXpro Tools 5.0 (Gepsoft 2014), a powerful soft computing software package, was employed to develop planning models based on the GEP. The core objective of the study is to explore the practicality of the GEP methodologies in predicting the surface mean pressure coefficient ($\bar{C}_p$). Thus, the foremost task was to determine the relevant testing and training data subset for constructing a predictive model and evaluating its performance. The data set used in this study was achieved by a small scale C-shaped building models experimented at the IIT Kharagpur (IITK). Previously, Swami and Chandra (1988) proposed an equation for calculating the mean pressure coefficient at surfaces of low-rise building. Further, Muehleisen and Patrizi (2013) developed the model for the mean pressure coefficient at a wall of a low-rise building by a various angle of incidence, θ and the side ratio D/B. In this study, GEP is adopted to obtain a model for the prediction of ($\bar{C}_p$) on the surface of C-shaped models which may be a function of overall side ratio with curvature (D/B) or side ratio without curvature (d/b), height ratio (D/H), curvature ratio (R/D), and wind incidence angle (θ) of the building model. Therefore, the dimensionless equation for $\bar{C}_p$ can be written as:

$$\bar{C}_p = f\left(\frac{d}{b}, \frac{D}{H}, \frac{R}{D}, \theta\right) \quad (4)$$

Here, the values of d/b, D/H, R/D and θ are taken as input variables to determine $\bar{C}_p$.

3.2 Modeling of $\bar{C}_p$ by using gene-expression programming (GEP)

The most popular database method from the machine-learning field is the gene-expression programming (GEP) which is adopted here to obtain a model for the prediction of mean $\bar{C}_p$ on the surface of C-shaped models. The process of GEP are encrypted into chromosomes organized in linear form to solve a particular problem, which are conveyed into an expression trees (ET) that are chosen according to their fitness at problem resolving stage (Ferreira 2001, 2002). The advantages of GEP are (Ferreira 2002): (i) the genes are in compressed linear form, relatively small, and easy to operate genetically (replicate, mutate, recombine, etc.); (ii) genes are selected through the reproduction with modification according to their fitness; and (iii) the complete appearance of generation of their respective genes into an expression trees. An algorithm involved in the process of GEP is shown briefly in the form of flowchart in Fig. 4.

Initially, the individual genes of the inhabitants are randomly generated, and then the genes are articulated and weighed based on a fitness function. In GEP modelling process, it is necessary to choose proper fitness function (E_i). There are various types of fitness function available in GEP for evaluating model performance that includes mean squared error (MSE), root mean squared error (RMSE), mean absolute error (MAE), relative squared error (RSE), root relative squared error (RRSE), relative absolute error (RAE), and others. The fitness (f_i) of an individual chromosome (i) is defined by the following expression

$$f_i = \frac{M}{1 + E_i} \quad (5)$$

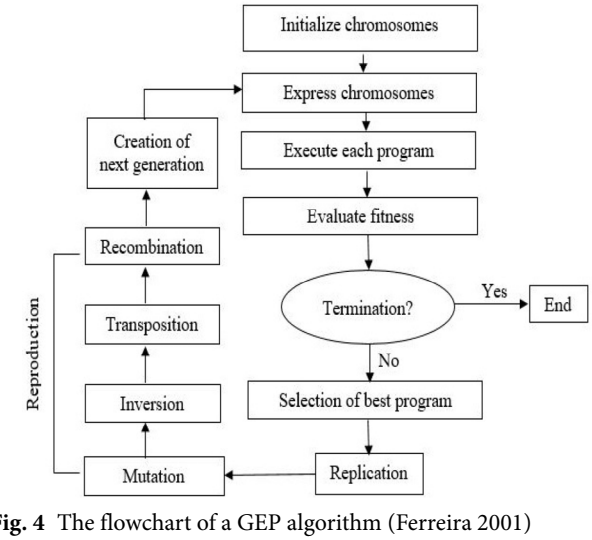

Fig. 4 The flowchart of a GEP algorithm (Ferreira 2001)

where M is the selection range which ranges between 0 and 1000 with 1000 corresponded to the ideal (Ferreira 2006) and E_i the fitness function. For this problem, the RMSE is used as the fitness function (E_i) of an individual chromosome (i), defined as

$$E_i = \sqrt{\frac{1}{N}\sum_{j=1}^{N}\left(P_{ij} - O_j\right)^2} \quad (6)$$

where N the total number of fitness cases or sample cases, P_{ij} the predicted value by the individual chromosome i for fitness case j, and O_j the object value for fitness case j. $\left|P_{ij} - O_j\right|$ gives the value of accuracy of the target. So, the E_i index ranges from 0 to infinity, with 0 corresponding to the ideal. The value of accuracy is equal to zero if $\left|P_{ij} - O_j\right| \leq 0.01$ and $f_i = f_{max} = M$.

In GEP another major problem is to choose an architecture of generation of chromosomes which includes the length of the head and tail size of chromosomes, random constants and the number of genes. The head size decides the maximum size of each term or complexity in the model. The number of genes per chromosome determines the number of fundamental terms in the models as each gene programmes for various subset model. The chromosomes may be single or multiple gene consisting of variables with mathematical operators or function set. Selection of appropriate function set for developing model is much important in GEP process. The mathematical operators may be arithmetic operators (+, −, ×, ÷) as well as functions (x^2, x^3, $\sqrt{x}$, $\sqrt[3]{x}$, e^x, $(1-x)$, $\ln(x)$, $\sin(x)$, $\cos(x)$, $\tan(x)$, power, etc.). The next step is to select the linking function for the subsets of model. Whenever the number of genes is greater than one, an appropriate linking function is required to attach the subset models programmed in each gene. Linking function may be the addition, subtraction, multiplication, division, average, min, or max which is used to link the subset of models. The final step is to choose the set of genetic operators (mutation, inversion, transposition, and recombination) and their rates that cause variation in model generation. Readers can refer to Ferreira (2001) for a detailed discussion on GEP by Mehdizadeh et al. (2016).

The terminals set are different combinations of input variables such as curvature ratio (R/D), side ratio without curvature (d/b), height ratio (D/H), and incidence angle (θ) in radian to create the chromosomes. There is no particular rule for the divisional process of training and testing data. Researchers have used different data division between testing and training that varies with problems. For the present modelling, different data divisions such as 60%–40%, 65%–35%, 70%–30%, 75%–25%, and 80%–20% between training and testing data that varies with problems and observed the best possible output results in terms of various statistical measures. Among all these data division process, 70%–30% gives best results i.e. for the present work, about 70% of data are used for training and the rest 30% for testing. A total of 208 numbers of data described (Tables 2 and 3) are used in modelling and distributed randomly for training and testing data phase.

Four basic arithmetic operators (+, −, ×, ÷) and basic mathematical functions such as x^2, $\sqrt{x}$, e^x, $1/x$, $\ln(x)$, $(1-x)$, are used for the development of the model. For present case RMSE was used as the fitness function and the fitness, f_i (Eq. (5)), returns the summation of error in the target value for which root mean square error (RMSE) (Eq. (6)) is calculated. For present study, M=1000 and, therefore, f_{max} = 1000.

Initially, the model was generated with a single gene and two head lengths. Further, the number of genes and heads were increased one at a time during each run and the performances of training and testing dataset are recorded. It was observed that the performances of training and testing data phase did not significantly improve for the head length greater than 8 and more than three genes. Therefore, eight as the head length, and three genes per chromosome were adopted for the development of GEP model. Addition operator was used as the linking function of three genes. A large number of generations (17505) are tested. After 17505 numbers of generations, there is no variation occurs for performances of training and testing phase i.e. the generations may stop at this stage. Various operating functions are used for predicting $\overline{C}_p$ in GEP modelling which are presented in Table 4 with their weight and arity. The important parameters that affect the performance of the GEP modelling which are used for the development of model for estimating $\overline{C}_p$ are presented in Table 5. In fact, the mentioned parameters are borderlines of the GEP which can affect the performance of the GEP. It must be said that all mentioned parameters are selected by the user using trial and error procedure to obtain

Table 4 Function set for development of GEP model

Function	Symbol	Weight	Arity
Addition	+	4	2
Subtraction	−	4	2
Multiplication	×	4	2
Division	/	1	2
Natural logarithm	$\ln(x)$	1	1
x to the power of 2	x^2	1	1
Inverse	$1/x$	1	1
x to the power of 3	x^3	1	1
Square root	sqrt	1	1
Complement	$(1-x)$	1	1

Table 5 Operational parameters used in GEP model

Description of parameter	Parameter setting
Linking function	Addition
Fitness function	RMSE
Program size	28
Literals	6
Number of generations	17505
Constants per gene	10
Data type	Floating point
Number of chromosomes	30
Head size	8
Number of genes	3
Gene size	26
Mutation rate	0.00138
Inversion rate	0.00546
Gene recombination rate	0.00277
One-point recombination rate	0.00277
Two-point recombination rate	0.00277
Gene transposition rate	0.00277
Insertion sequence (IS) transposition rate	0.00546
Root insertion sequence (RIS) transposition rate	0.00546

the optimum structure of the GEP. Ability in presenting algebraic equations between output and input variables is nobility characteristic of the GEP which is very important in the prediction process.

The architecture of GEP is flexible that allows to create a multiple number of models of various gene sizes and shapes. At first, a small population of models are generated arbitrarily and further the performances of model for each data are tested. By seeing the performance or fitness, the models are selected or reproduce with minor changes, giving rise to a formation of new models. These processes of selection and reproduction are repeated until a desired solution is achieved on a predefined number of generations, leading to the finding an optimum model. If the satisfactory quality of the solution is found, evolution process stops, and the best-obtained solution at this stage is reported. But if stop conditions are not found, the best solution for the present generation is kept unchanged. The process is repeated for a certain number of generations, and the solution arrives. The optimum model for predicting the surface mean pressure coefficient ($\overline{C}_p$) for the C-shaped building is described as

$$\overline{C}_p = 0.14 + \frac{(1-\theta)\times(R/D+1.57)}{\left((\theta-1.15)^2\times(R/D+1.57)\right)+1} + \left(\frac{5.06}{d/b} - \frac{9.88}{D/H}\right)\times\left(\frac{d/b}{69.56}\right) \quad (7)$$

By putting $d = (D-R)$ and $b = (B-R)$, Eq. (7) can be written as:

$$\overline{C}_p = 0.14 + \frac{(1-\theta)\times(R/D+1.57)}{\left((\theta-1.15)^2\times(R/D+1.57)\right)+1} + \left(\frac{5.06}{(D-R)/(B-R)} - \frac{9.88}{D/H}\right)\times\left(\frac{(D-R)/(B-R)}{69.56}\right) \quad (8)$$

where θ = angle of incidence, R = radius of curvature, D = overall depth, d = depth, B = overall breath, b = breath, and H = height. Figure 5 describes expression trees of the superior scenarios.

An expression tree (ET) representation as in Eq. (8) is shown in Fig. 5, which represents GEP model for estimating $\overline{C}_p$. In Fig. 5, d1 represents d/b, d2 represents D/H, d3 represents R/D, and d4 represents θ (radian). C1 and C2 represent the numerical constants used in the 1st gene of the model. C4 and C5 represent the constant used in the 2nd gene of the model. Similarly, C8 and C9 represent the constants used in the 3rd gene of the model.

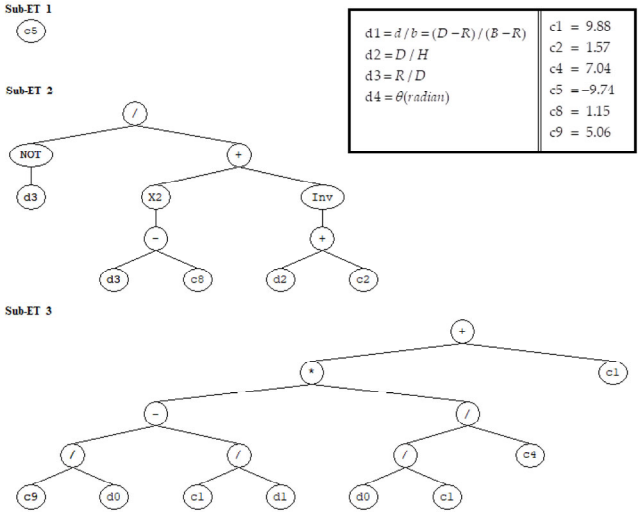

Fig. 5 Expression tree of the superior scenario of the C-shaped building model

4 Results and discussion

After the development of the model (Eq. (8)), an attempt has been made for testing its strength. A comparison (Fig. 6) is made between the predicted values of $\overline{C}_p$ using the developed model equation (Eq. (8)) and the corresponding observed values of $\overline{C}_p$.

It is seen from Fig. 6 that the predicted values of $\overline{C}_p$ agree fairly well with the corresponding observed ones. The authors have also compared the predicted results by the GEP model with the values obtained using different equations (Eqs. (2) and (3)) on the surfaces of the building models. The comparisons of the experimental values of surface mean pressure coefficient $\overline{C}_p$ (with the angle of incidence) with

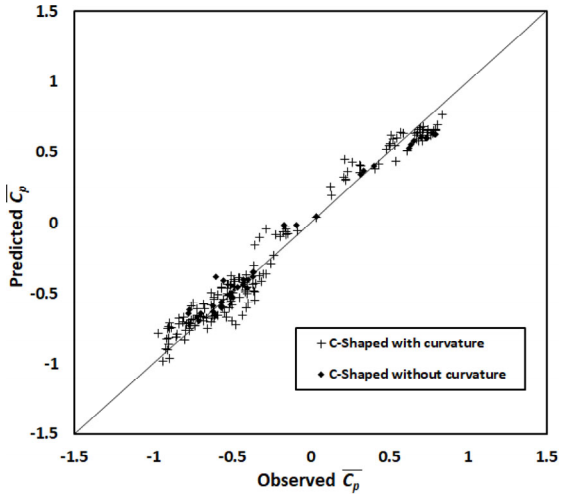

Fig. 6 Comparison between predicted and experimental values of $\overline{C}_p$

those obtained from different equations including the authors' developed equation are shown in Figs. 7 to 11. Here the authors have tried to show the curvature effect on $\overline{C}_p$ by varying the side ratio. In the 1st case, the variation of $\overline{C}_p$ with the angle of incidence for different curvatures are shown (Figs. 7(a) to 7(d)) by maintaining the side ratio, D/B as 1 and height ratio, D/H as 0.67. In the 2nd case, height ratio (D/H) and curvature ratio (R/D) are kept constant and variation of $\overline{C}_p$ with angle of incidence (θ) for different side ratios, i.e., D/B, and d/b are shown in Figs. 8(a) to 8(d). In the 3rd case, height ratio (D/H) and curvature ratio (R/D) are kept constant and variation of $\overline{C}_p$ with angle of incidence (θ) for different frontal ratios, i.e., D/B, and d/b are shown in Figs. 9(a) to 9(d). In the 4th case, the variation of $\overline{C}_p$ with angle of incidence are shown for different height ratio (Figs. 10(a) to 10(d)) by maintaining the side ratios (D/B, d/b) and curvature ratio (R/D) constant as 1, 1.5, and 0.5 respectively. Finally in the 5th case, the variation of $\overline{C}_p$ with angle of incidence of different C-shaped buildings not having corner curvature, varying with side ratio (D/B) and height ratio (D/H) are shown in Figs. 11(a) to 11(c).

Case I: Variation of surface mean pressure coefficient ($\overline{C}_p$) with angle of incidence (θ) for different curvature ratios

Figures 7(a) to 7(d) express $\overline{C}_p$ for the surface 1 (a front face) of the model as a function of the wind angle of incidence θ. It can be seen that the prediction obtained by the GEP model and the corresponding observed data are agreed well with the S&C equation in the entire range of incidence angles. But the M&P equation prediction it agrees closely with the GEP and observed data in a lower range of wind incidence

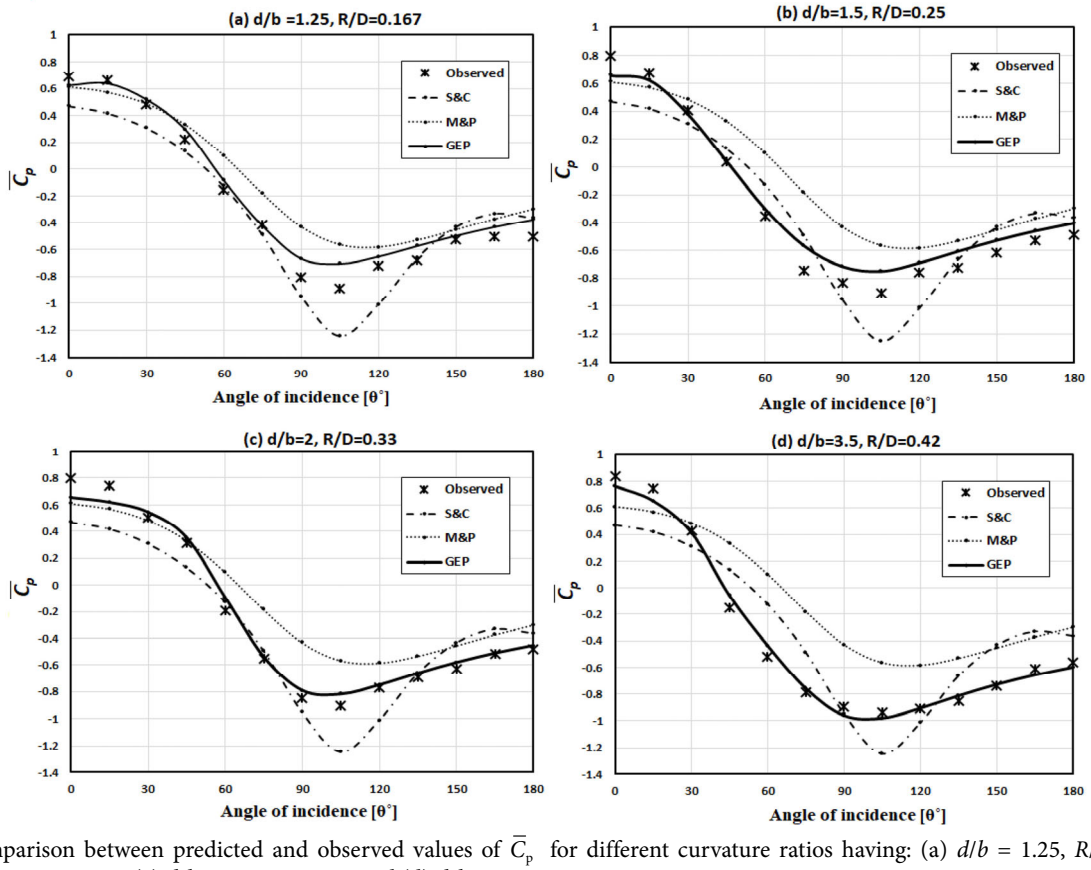

Fig. 7 Comparison between predicted and observed values of $\overline{C}_p$ for different curvature ratios having: (a) d/b = 1.25, R/D = 0.167; (b) d/b = 1.5, R/D = 0.25; (c) d/b = 2, R/D = 0.33; and (d) d/b =3.5, R/D = 0.42

angle i.e., 0° to 90° and higher range 120° to 180°. In the middle range of wind incidence angle (90° to 120°) M&P equation data deviates from those of GEP and S&C data. M&P executes usually better than S&C, as stated by Muehleisen and Patrizi (2013). Comparison of the data obtained by the GEP model and the other two models authenticate the GEP model and its effectiveness to forecast $\overline{C}_p$ for entire series of wind incidence angle.

Case II: Variation of surface mean pressure coefficient ($\overline{C}_p$) with angle of incidence (θ) for different side ratios

Figures 8 (a) to 8(d) show $\overline{C}_p$ towards surface 1 for different side ratios D/B and d/b as a function of the wind angle of incidence θ. Here also, GEP unveils the correctness of the calculated data for any D/B and θ; and contributes a best prediction of the calculated data. GEP prediction is more close to the observed data in all the cases. Predictions obtained by GEP model and the corresponding observed data are in close agreement with the S&C outputs in the entire range of incidence angles. As in the first case, M&P equation predictions are in close agreement with others only in the lower range of wind incidence angle i.e., 0° to 90° and higher range 120° to 180°. But in the middle range of wind incidence angle (90° to 120°), M&P deviates from those of GEP and S&C data.

Case III: Variation of surface mean pressure coefficient ($\overline{C}_p$) with angle of incidence (θ) for different frontal ratios

Figures 9(a) to 9(d) show $\overline{C}_p$ on surface 1 for different frontal ratios D/B and d/b as a function of the wind angle of incidence θ. Here also, GEP produces the good correlation of the measured data for any D/B and θ; and finds an accurate prediction of the measured data. GEP prediction is more close to the observed data in all the cases. Predictions obtained by GEP model and the corresponding observed data are in close agreement with the S&C in the entire range of incidence angles. As in the first case, M&P equation predictions are in close agreement with others only in the lower range of wind incidence angle i.e., 0° to 90° and higher range 120° to 180°. But in the middle range of wind incidence angle (90° to 120°), M&P deviates from those of GEP and S&C data.

Case IV: Variation of surface mean pressure coefficient ($\overline{C}_p$) with angle of incidence (θ) for different height ratios

Figures 10(a) to 10(d) show $\overline{C}_p$ for the surface 1 of the model as a utility of the wind incidence angle θ. It can be seen that predictions of $\overline{C}_p$ by developed GEP model and

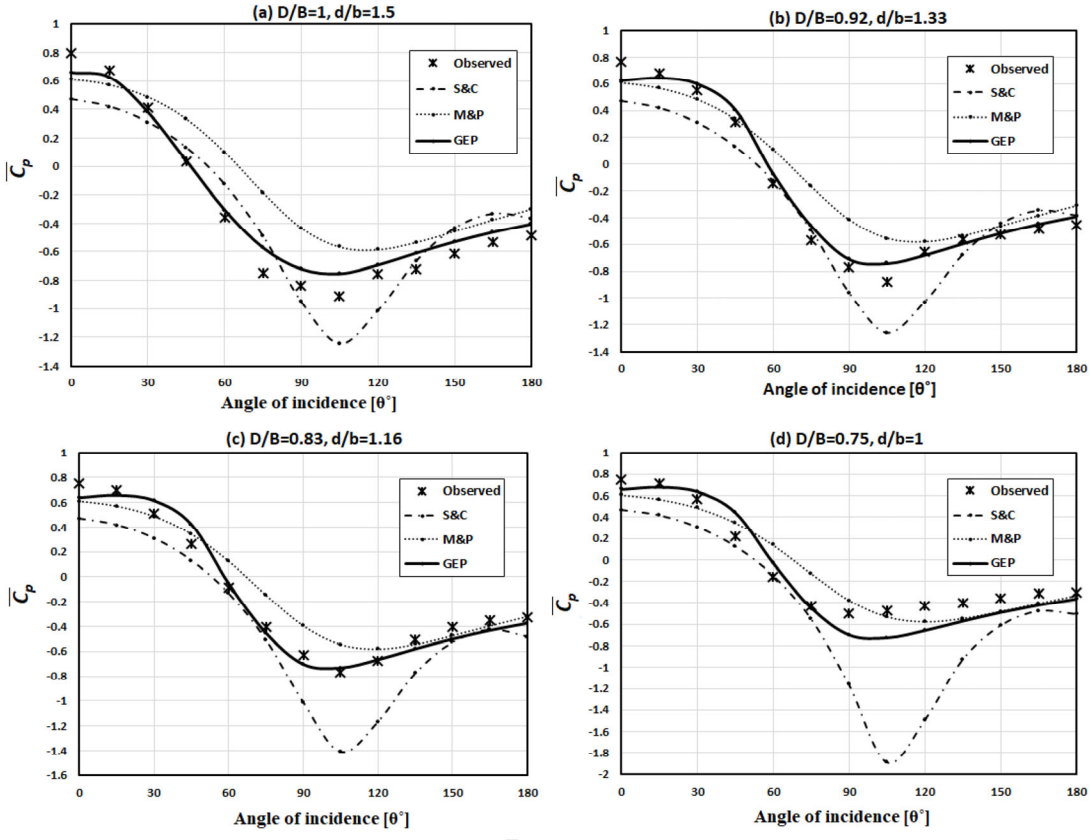

Fig. 8 Comparison between predicted and observed values of $\overline{C}_p$ for different side ratios having: (a) D/B = 1, d/b = 1.5; (b) D/B = 0.92, d/b = 1.33; (c) D/B = 0.83, d/b = 1.16; and (d) D/B = 0.75, d/b = 1

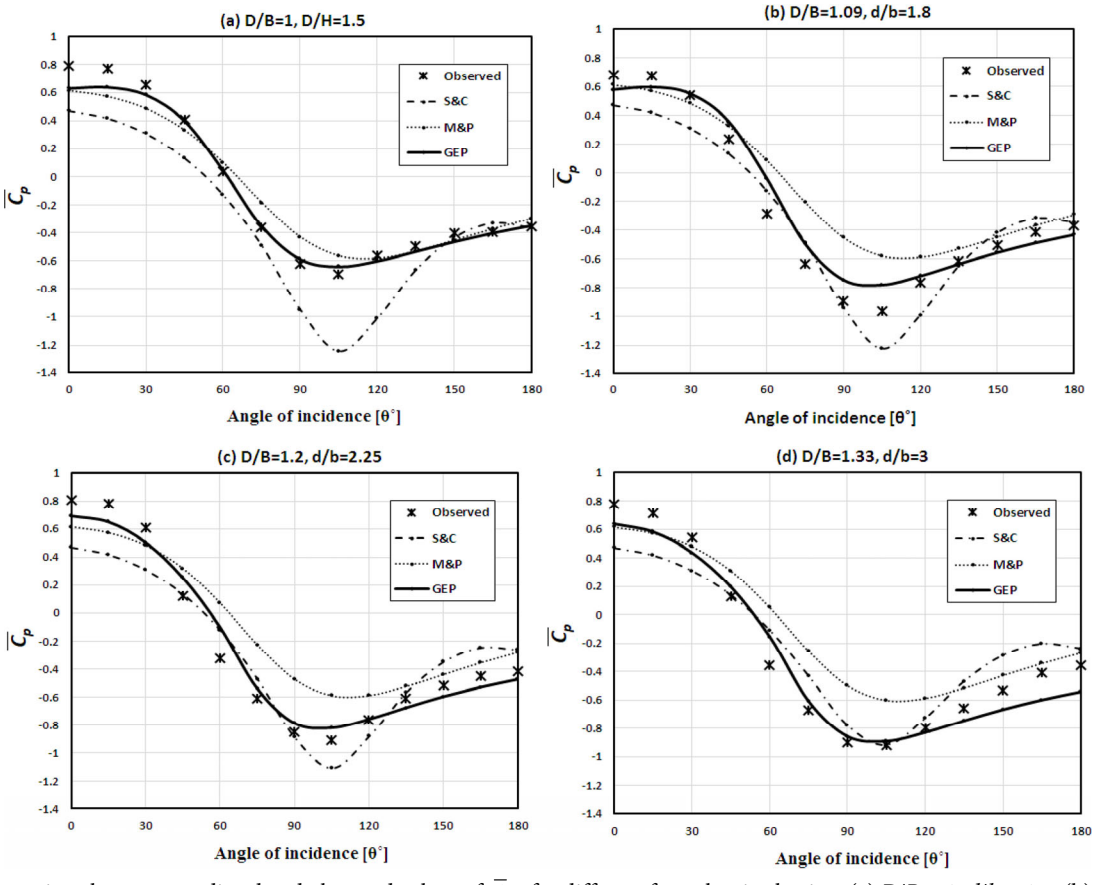

Fig. 9 Comparison between predicted and observed values of $\overline{C}_p$ for different frontal ratios having: (a) D/B = 1, d/b = 1.5; (b) D/B = 1.09, d/b = 1.8; (c) D/B =1.2, d/b =2.25; and (d) D/B =1.33, d/b =3

other two S&C and M&P equations agree well with observed data in a lower range of angle of incidence (0° to 60°) and again beyond 150°. The predictions by M&P model in the middle range of angle of incidence (90° to 120°) deviates from others, but predictions by GEP is in close agreement with observed data and with the S&C predictions in the entire range of angle of incidence.

Case V: Variation of surface mean pressure coefficient ($\overline{C}_p$) with angle of incidence (θ) for without corner curvature

Figures 11(a) to 11(c) show $\overline{C}_p$ value of the wind incidence angle θ for the surface 1 of the C-shaped model without corner curvature. Three different types of C-shaped models with zero curvature are investigated by varying side ratios (D/B) and height ratios (D/H). It can be seen that predictions of $\overline{C}_p$ by developed GEP model agree well with observed data when compared with S&C and M&P equations.

Testing of model performance is crucial after its development where comparisons between the observed (O_i) and the predicted (P_i) values should give the minimum error between the values. Performance of all the models are demonstrated through their standard statistical error calculations such as the coefficient of determination (R^2), root mean square error (RMSE), mean absolute error (MAE), and the mean absolute percentage error (MAPE). The value of R^2, RMSE, MAE, and MAPE are considered to find the adequacy of the model concerning the dataset (Gandomi et al. 2013; Mentaschi et al. 2013; Najafzadeh and Azamathulla 2013; Ebtehaj et al. 2015; Najafzadeh and Lim 2015). These parameters are evaluated by the following equations given as:

$$R^2 = \left[\frac{\sum_{i=1}^{N}(P_i-\overline{P})(O_i-\overline{O})}{\sqrt{\sum_{i=1}^{N}(P_i-\overline{P})^2\sum_{i=1}^{N}(O_i-\overline{O})^2}}\right]^2 \quad (9)$$

$$\text{MAE} = \frac{\sum_{i=1}^{N}|P_i-O_i|}{N} \quad (10)$$

$$\text{RMSE} = \sqrt{\frac{\sum_{i=1}^{N}(P_i-O_i)^2}{N}} \quad (11)$$

$$\text{MAPE} = \frac{\sum_{i=1}^{N}\left(\frac{P_i-O_i}{P_i}\times 100\right)}{N} \quad (12)$$

where, P_i is the i^{th} estimated $\overline{C}_p$ using GEP, O_i the i^{th} observed $\overline{C}_p$, $\overline{P}$ the average of the estimated $\overline{C}_p$ values, $\overline{O}$ the

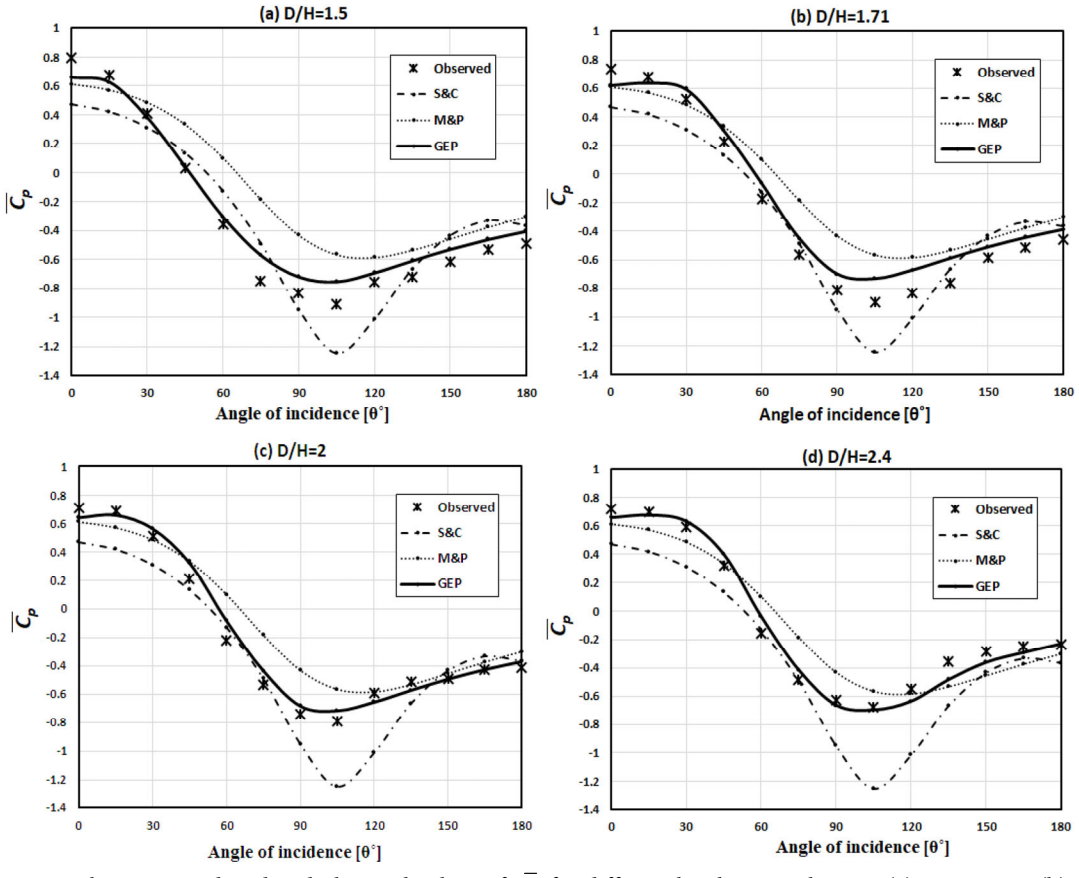

Fig. 10 Comparison between predicted and observed values of $\overline{C}_p$ for different height ratios having: (a) D/H = 1.5; (b) D/H = 1.71; (c) D/H = 2; and (d) D/H = 2.4

average of the observed $\overline{C}_p$ values and N the number of observations.

The closure is the value of R^2 to 1 indicates a well correlation among the observed and the predicted value of the various model. MAE measures the closeness of the predicted and observed value, while RMSE shows the deviation of a predicted value from observed value. MAE and RMSE have the unit similar to the dependent input value, i.e., a lower value of predictive variables depicts a better prediction model (Mohanta et al. 2018).

Table 6 shows the error analysis of present experimental dataset with different predictive models. From the analysis, we can conclude that the GEP model gives better predictions of pressure coefficient on the surface of the C-shaped model as compared to other model outputs with minimum error. The lowest values of RMSE and MAE as 0.1 and −6.73 indicate the good performance of the model. Value of R^2 = 0.97 shows a good correlation between the observed and the predicted value of the GEP model as compared to S&C (R^2 = 0.86) and M&P (R^2 = 0.91). The error analysis indicates the acceptability of the GEP model for its practical application.

The values of MAE and RMSE have same unit equal to the predicted values. For the better understanding of the MAE and RMSE, they can be normalized with the difference of the maximum $\overline{C}_p$ and minimum $\overline{C}_p$ values for the corresponding datasets given as:

$$\mathrm{NMAE}(\%) = \frac{\mathrm{MAE}}{\max(\overline{C}_p) - \min(\overline{C}_p)} \times 100 \tag{13}$$

$$\mathrm{NRMSE}(\%) = \frac{\mathrm{RMSE}}{\max(\overline{C}_p) - \min(\overline{C}_p)} \times 100 \tag{14}$$

where NMAE and NRMSE stand for Normalized MAE and RMSE respectively. Figure 12 showed the normalized values of MAE and RMSE for differential equations and developed GEP model for predicting $\overline{C}_p$ value of the calibrated dataset.

4.1 Validation of the developed model with TPU dataset

The experimental C-shaped building models are considered for the development of equation for surface mean pressure coefficient ($\overline{C}_p$) (Eq. (8)) by GEP approach. Now, authors have chosen the data of flat roof building models named as TPU Data (Appendix A, Tables A1 and A2) measured at Wind Engineering Information Centre, Tokyo Polytechnic

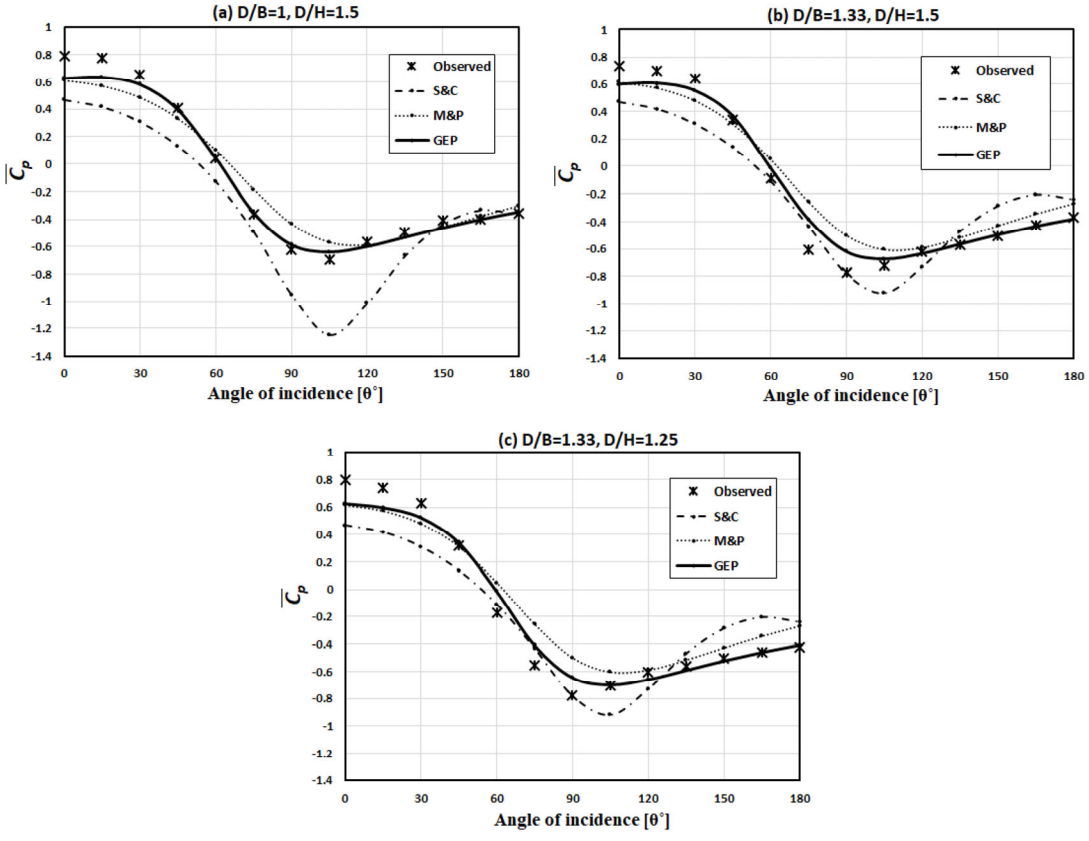

Fig. 11 Comparison between predicted and observed values of $\overline{C}_p$ for models without any corner curvature having: (a) D/B = 1, D/H = 1.5; (b) D/B = 1.33, D/H = 1.5; and (c) D/B = 1.33, D/H =1.25

Table 6 Error analysis of predicted $\overline{C}_p$ by GEP against reported models for experimental data

Models	S&C	M&P	GEP
ME (%)	−9.17	−23.44	−3.36
R^2	0.86	0.91	0.97
MAE	0.20	0.18	0.08
RMSE	0.23	0.22	0.10
MAPE (%)	−9.36	−19.54	−6.73

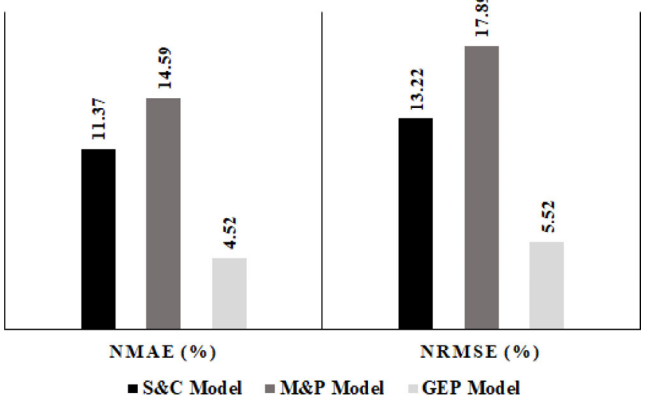

Fig. 12 Comparison of NMAE and NRMSE value for developed GEP model with S&C and M&P equation for predicting $\overline{C}_p$ value

University (Bre et al. 2018) for the applicability and suitability of developed GEP model. The TPU data of five building models of varying wind angles, side ratios (d/b = D/B = 1, 0.4, 0.667, 1.5 and 2.5) and height ratios (H/B = 1/4, 2/4, 3/4 and 4/4) are used for comparison. The $\overline{C}_p$ values for wind angles (θ) from 0° to 180° at 15° intervals are calculated by using the developed GEP model (Eq. (8)) and compared with corresponding TPU data in Fig. 13.

The error analysis is also performed regarding mean percentage error (ME), standard deviation (SD) to mean, coefficient of determination (R^2), mean absolute error (MAE), root mean square error (RMSE) and mean absolute percentage error (MAPE) on surface 1 to show the goodness of the model.

The overall percentage of mean error for TPU data set is 9.19% with a standard deviation of 45.25. The value of R^2 for overall TPU dataset is 0.97. Similarly, the value of MAE, RMSE, and MAPE are found to be 0.073, 0.089 and −7.76% respectively. Variation of mean percentage error (ME) on the frontal surface of TPU dataset by varying D/B, D/H and their standard deviations (SD) are shown in Fig. 14. The individual error analysis regarding R^2, MAE, RMSE, and MAPE on the frontal surface for various D/B and D/H model of TPU dataset are shown in Table 7.

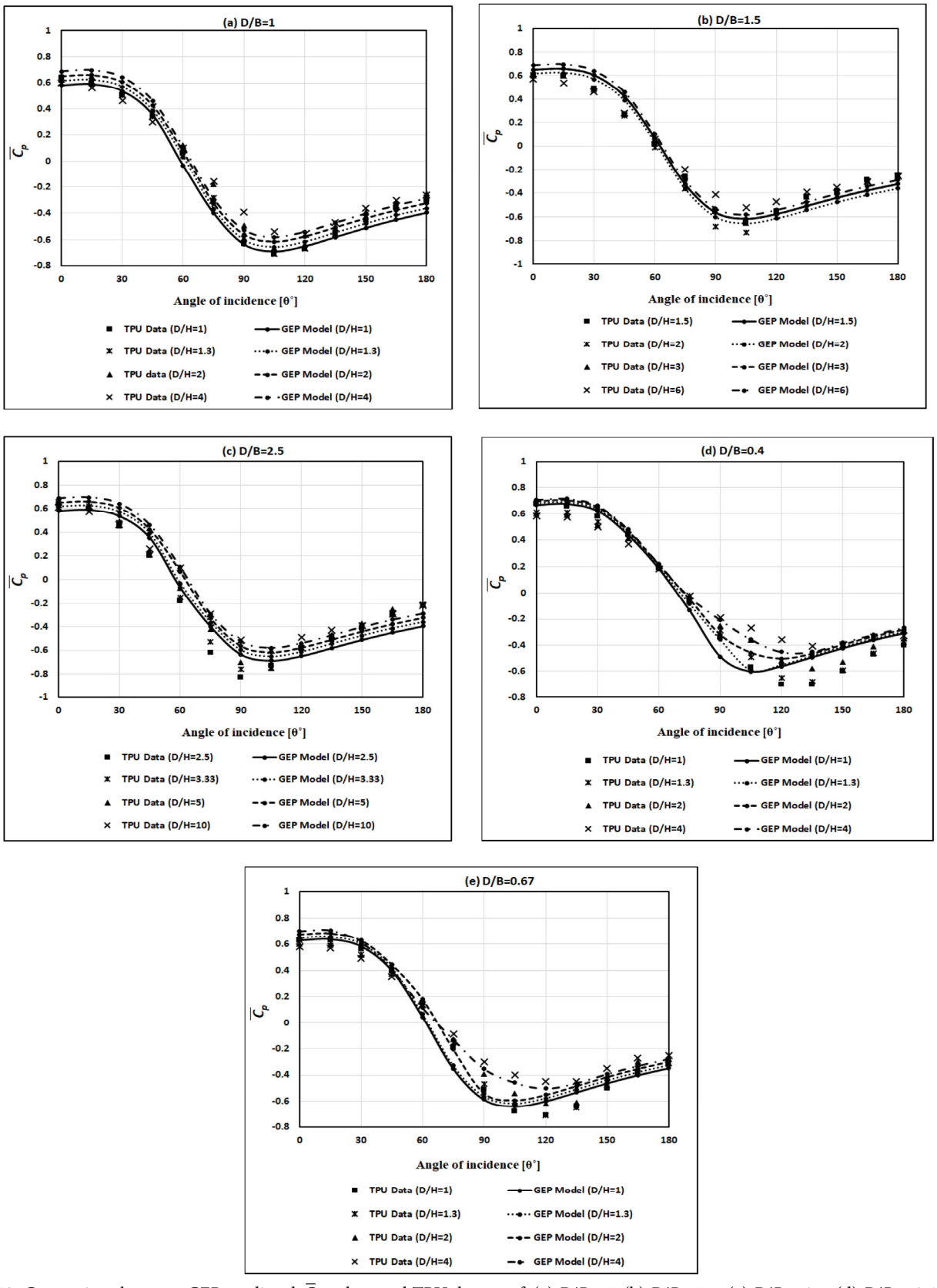

Fig. 13 Comparison between GEP predicted $\overline{C}_p$ values and TPU dataset of: (a) D/B =1; (b) D/B =1.5; (c) D/B = 2.5; (d) D/B = 0.4; and (e) D/B = 0.67

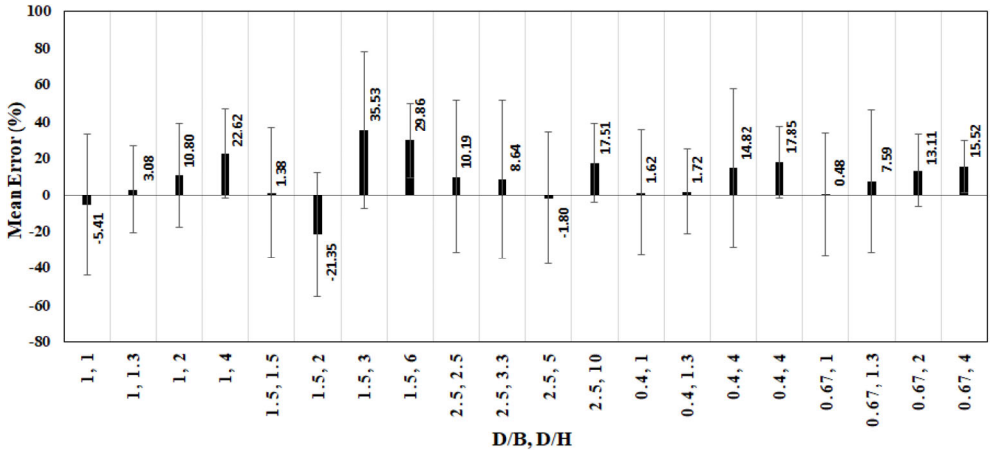

Fig. 14 Variation in mean percentage error and standard deviation for various D/B and D/H model of TPU dataset

Table 7 Error analysis of predicted $\overline{C}_p$ data using the GEP model with TPU dataset

D/B	D/H	R^2	MAE	RMSE	MAPE
1	1	0.991	0.046	0.057	5.65
1	1.3	0.988	0.047	0.054	−1.56
1	2	0.981	0.061	0.071	−6.70
1	4	0.983	0.078	0.099	−2.38
1.5	1.5	0.980	0.061	0.071	−16.37
1.5	2	0.980	0.060	0.072	−36.86
1.5	3	0.987	0.067	0.076	16.12
1.5	6	0.994	0.094	0.107	4.88
2.5	2.5	0.935	0.111	0.126	−15.57
2.5	3.3	0.947	0.102	0.114	−14.99
2.5	5	0.960	0.093	0.106	−20.96
2.5	10	0.988	0.066	0.091	5.75
0.4	1	0.968	0.080	0.104	−19.26
0.4	1.3	0.970	0.089	0.103	−11.13
0.4	2	0.976	0.078	0.088	−15.61
0.4	4	0.990	0.072	0.088	−2.22
0.67	1	0.978	0.056	0.075	−6.73
0.67	1.3	0.968	0.072	0.088	−8.15
0.67	2	0.979	0.068	0.079	−6.94
0.67	4	0.996	0.062	0.073	−2.16

5 Conclusions

Gene-expression programming (GEP) uses a fixed-length gene expression representation to encode computer programs, and be able to find concise and readable solution efficiently. In this research, the GEP is used to predict the surface mean pressure coefficient ($\overline{C}_p$) for all the cases of wind angles of incidence, curvature ratio, aspect ratio and also for the models without curvature. The GEP model is capable of predicting the surface mean pressure coefficient ($\overline{C}_p$) with high accuracy. It is pertinent to mention that the proposed GEP model is based on laboratory datasets with dimensionless geometric parameters in the ranges; $0.75 \le D/B \le 1.33$, $1 \le d/b \le 3.5$, $1.5 \le D/H \le 2.4$, $0.17 \le R/D \le 0.42$ and $0° \le \theta \le 180°$. From the present analysis, the following conclusions are drawn for estimating surface mean pressure coefficient ($\overline{C}_p$) on the frontal surface of C-shaped building models:

- The predictions of surface mean pressure coefficient ($\overline{C}_p$) values obtained by using developed model fit fairly well with the corresponding experimental ones.
- The predicted values using the developed model compares well with those obtained from S&C and M&P models for low rise square shaped buildings. Thus, indicating the utility of the developed model for rectangular models as well.
- The developed GEP model is found compatible with the actual TPU dataset.
- The mean absolute error and root mean square error of the predicted results by the GEP model is less as compared to predictions by both S&C and M&P models. This indicates that the proposed model predicts surface mean pressure coefficient more close to the experimental data, i.e. more accurate than those by using S&C and M&P models.
- The results give a clear suggestion of the efficiency of the developed GEP model and its potential use for practical applications within a similar range of non-dimensional parameter tested in this work.
- The present study clearly indicates that the GEP model is more useful for any condition without limitations.

Acknowledgements

The authors express a deep sense of gratefulness to Head of the Department of Aerospace Engineering, Indian Institute of Technology Kharagpur, India for permitting and providing facilities to carry out the experiments.

Appendix A

Table A1 C_p as a function of wind angle θ, side ratio D/B, and height ratio D/H from Tokyo low-rise wind tunnel database measurements on sides 1 and 3

D/B	D/H	0°	15°	30°	45°	60°	75°	90°	105°	120°	135°	150°	165°	180°
1	1	0.64	0.6	0.51	0.34	0.06	−0.31	−0.63	−0.71	−0.67	−0.55	−0.45	−0.36	−0.31
1	1.3	0.63	0.61	0.5	0.34	0.08	−0.28	−0.59	−0.71	−0.67	−0.56	−0.43	−0.34	−0.28
1	2	0.62	0.65	0.51	0.35	0.12	−0.18	−0.49	−0.66	−0.66	−0.51	−0.39	−0.32	−0.25
1	4	0.6	0.56	0.46	0.3	0.1	−0.16	−0.39	−0.54	−0.56	−0.47	−0.36	−0.3	−0.26
1.5	1.5	0.62	0.6	0.5	0.29	−0.06	−0.46	−0.71	−0.73	−0.63	−0.51	−0.45	−0.33	−0.25
1.5	2	0.61	0.6	0.48	0.26	−0.01	−0.36	−0.68	−0.73	−0.6	−0.49	−0.43	−0.31	−0.25
1.5	3	0.6	0.6	0.49	0.27	0.02	−0.26	−0.55	−0.65	−0.55	−0.43	−0.38	−0.29	−0.25
1.5	6	0.57	0.54	0.46	0.28	0.06	−0.2	−0.41	−0.52	−0.47	−0.39	−0.35	−0.3	−0.26
2.5	2.5	0.64	0.6	0.45	0.2	−0.18	−0.62	−0.83	−0.73	−0.58	−0.51	−0.41	−0.3	−0.22
2.5	3.3	0.66	0.62	0.48	0.21	−0.15	−0.53	−0.76	−0.75	−0.58	−0.48	−0.39	−0.28	−0.21
2.5	5	0.63	0.62	0.49	0.24	−0.07	−0.42	−0.7	−0.75	−0.58	−0.47	−0.37	−0.25	−0.22
2.5	10	0.61	0.57	0.46	0.26	0	−0.29	−0.51	−0.6	−0.49	−0.43	−0.39	−0.29	−0.22

Note: The wind angle θ is measured from the normal to side 1. D is the length of sides 2 and 4 and B is the length of sides 1 and 3.

Table A2 C_p as a function of wind angle θ, side ratio D/B, and height ratio D/H from Tokyo low-rise wind tunnel database measurements on sides 1 and 3

D/B	D/H	0°	15°	30°	45°	60°	75°	90°	105°	120°	135°	150°	165°	180°
0.4	1	0.68	0.66	0.58	0.44	0.19	−0.07	−0.34	−0.57	−0.7	−0.7	−0.6	−0.47	−0.4
0.4	1.3	0.61	0.61	0.54	0.41	0.18	−0.06	−0.29	−0.49	−0.65	−0.68	−0.59	−0.46	−0.38
0.4	2	0.6	0.59	0.51	0.41	0.2	−0.02	−0.25	−0.36	−0.52	−0.58	−0.53	−0.41	−0.35
0.4	4	0.58	0.57	0.5	0.37	0.18	−0.02	−0.19	−0.27	−0.36	−0.41	−0.4	−0.34	−0.33
0.67	1	0.63	0.63	0.56	0.4	0.15	−0.19	−0.51	−0.68	−0.71	−0.64	−0.5	−0.38	−0.31
0.67	1.3	0.63	0.59	0.52	0.37	0.14	−0.15	−0.47	−0.61	−0.71	−0.65	−0.48	−0.35	−0.31
0.67	2	0.6	0.6	0.52	0.4	0.16	−0.13	−0.39	−0.54	−0.62	−0.61	−0.42	−0.3	−0.28
0.67	4	0.58	0.57	0.49	0.35	0.14	−0.09	−0.3	−0.4	−0.45	−0.45	−0.35	−0.27	−0.25

Note: The wind angle θ is measured from the normal to side 1. D is the length of sides 2 and 4 and B is the length of sides 2 and 4.

References

Ahmad S, Kumar K (2001). Interference effects on wind loads on low-rise hip roof buildings. *Engineering Structures*, 23: 1577–1589.

Akins RE (1976). Wind Pressures on Buildings. CER76-77EA-JEC15, Fluid Dynamics and Diffusion Laboratory, Colorado State University, USA.

Amin JA, Ahuja AK (2008). Experimental study of wind pressures on irregular plan shape buildings. In: Proceedings of BBAA VI International Colloquium on Bluff bodies Aerodynamics and Applications, Milano, Italy.

Amin JA, Ahuja AK (2011). Experimental study of wind-induced pressures on buildings of various geometries. *International Journal of Engineering, Science and Technology*, 3(5): 1–9.

Azamathulla HM, Ahmad Z, Ghani AA (2013). An expert system for predicting Manning's roughness coefficient in open channels by using gene expression programming. *Neural Computing and Applications*, 23: 1343–1349.

Babovic V, Keijzer M (2002). Rainfall runoff modelling based on genetic programming. *Hydrology Research*, 33: 331–346.

Bhattacharyya B, Dalui SK, Ahuja AK (2014). Wind induced pressure on E plan shaped tall buildings. *Jordon Journal of Civil Engineering*, 8(2): 120–134.

Bhattacharyya B, Dalui SK (2018). Investigation of mean wind pressures on E plan shaped tall building. *Wind and Structures*, 26(2): 99–114.

Bre F, Gimenez JM, Fachinotti VD (2018). Prediction of wind pressure coefficients on building surfaces using artificial neural networks. *Energy and Buildings*, 158: 1429–1441.

Chakraborty S, Dalui SK, Ahuja AK (2013). Experimental and numerical study of surface pressure on '+' plan shape tall building. *International Journal of Construction Materials and Structures*, 1: 45–58.

Chakraborty S, Dalui SK, Ahuja AK (2014). Wind load on irregular plan shaped tall building—A case study. *Wind and Structures*, 19: 59–73.

Cook NJ (1990). The designer's Guide to Wind Loading of Building Structures. Part 2: Static Structures. London: Butterworths (for) Building Research Establishment.

Cook N (2007). Designers' Guide to EN 1991-1-4 Eurocode 1: Actions on structures, general actions part 1-4. Wind actions. London: Thomas Telford Publishing.

Cóstola D, Blocken B, Hensen JLM (2009). Overview of pressure coefficient data in building energy simulation and airflow network programs. *Building and Environment*, 44: 2027–2036.

Cóstola D, Blocken B, Ohba M, Hensen JLM (2010). Uncertainty in airflow rate calculations due to the use of surface-averaged pressure coefficients. *Energy and Buildings*, 42: 881–888.

Cousin N, Savic DA (1997). A rainfall-runoff model using genetic programming. Centre for Systems and Control Engineering. Report No. 97, 3.

Crawley DB, Lawrie LK, Winkelmann FC, Buhl WF, Huang YJ, Pedersen CO, Strand RK, Liesen RJ, Fisher DE, Witte MJ, Glazer J (2001). EnergyPlus: Creating a new-generation building energy simulation program. *Energy and Buildings*, 33: 319–331.

Das BS, Devi K, Khatua KK (2019). Prediction of discharge in converging and diverging compound channel by gene expression programming. *ISH Journal of Hydraulic Engineering*, https://doi.org/10.1080/09715010.2018.1558116

Drecourt J-P (1999). Application of neural networks and genetic programming to rainfall runoff modeling. D2K Technical Report 0699-1-1, Danish hydraulic institute, Denmark.

Ebtehaj I, Bonakdari H, Zaji AH, Azimi H, Khoshbin F (2015). GMDH-type neural network approach for modeling the discharge coefficient of rectangular sharp-crested side weirs. *Engineering Science and Technology, an International Journal*, 18: 746–757.

Ferreira C (2001). Gene expression programming: A new adaptive algorithm for solving problems. *Complex Systems*, 13: 87–129.

Ferreira C (2002). Gene expression programming in problem solving. In: Roy R, Köppen M, Ovaska S, Furuhashi T, Hoffmann F (eds), Soft Computing and Industry. London: Springer.

Ferreira C (2006). Gene Expression Programming: Mathematical Modeling by an Artificial Intelligence. Berlin: Springer-Verlag.

Gandomi AH, Yun G, Alavi AH (2013). An evolutionary approach for modeling of shear strength of RC deep beams. *Materials and Structures*, 46: 2109–2119.

Gepsoft (2014). GeneXpro Tools Version 5.0.

Ginger JD, Letchford CW (1999). Net pressures on a low-rise full-scale building. *Journal of Wind Engineering and Industrial Aerodynamics*, 83: 239–250.

Giustolisi O (2004). Using genetic programming to determine Chèzy resistance coefficient in corrugated channels. *Journal of Hydroinformatics*, 6: 157–173.

Gomes MG, Moret Rodrigues A, Mendes P (2005). Experimental and numerical study of wind pressures on irregular-plan shapes. *Journal of Wind Engineering and Industrial Aerodynamics*, 93: 741–756.

Grosso M (1992). Wind pressure distribution around buildings: A parametrical model. *Energy and Buildings*, 18: 101–131.

Guven A, Gunal M (2008). Genetic programming approach for prediction of local scour downstream of hydraulic structures. *Journal of Irrigation and Drainage Engineering*, 134: 241–249.

Guven A, Aytek A (2009). New approach for stage–discharge relationship: gene-expression programming. *Journal of Hydrologic Engineering*, 14: 812–820.

Harris EL, Babovic V, Falconer RA (2003). Velocity predictions in compound channels with vegetated floodplains using genetic programming. *International Journal of River Basin Management*, 1: 117–123.

Ho TCE, Surry D, Davenport AG (1990). The variability of low building wind loads due to surrounding obstructions. *Journal of Wind Engineering and Industrial Aerodynamics*, 36: 161–170.

Karimi S, Shiri J, Kisi O, Shiri AA (2016). Short-term and long-term streamflow prediction by using 'wavelet–gene expression' programming approach. *ISH Journal of Hydraulic Engineering*, 22: 148–162.

Kim YC, Kanda J (2013). Wind pressures on tapered and set-back tall buildings. *Journal of Fluids and Structures*, 39: 306–321.

Li Y, Li Q (2016). Across-wind dynamic loads on L-shaped tall buildings. *Wind and Structures*, 23: 385–403.

Lin N, Letchford C, Tamura Y, Liang B, Nakamura O (2005). Characteristics of wind forces acting on tall buildings. *Journal of Wind Engineering and Industrial Aerodynamics*, 93: 217–242.

Lou W, Jin H, Chen Y, Cao L, Yao J (2005). Wind tunnel test study on wind load characteristics for double-skin facade building with rectangular shape. *Journal of Building Structure*, 26(1): 65–70. (in Chinese)

Lu S-l, Chen S-f, Li J-h, Jiao Y-f (2007). Numerical study on the effects of curved annex on the wind loads on a spherical tall building. *Engineering Mechanics*, 24(2): 115–119. (in Chinese)

MacDonald AJ (1975). Wind Loading on Buildings. London: John Wiley & Sons.

Mehdizadeh S, Behmanesh J, Khalili K (2016). Comparison of artificial intelligence methods and empirical equations to estimate daily solar radiation. *Journal of Atmospheric and Solar-Terrestrial Physics*, 146: 215–227.

Mehdizadeh S, Behmanesh J, Khalili K (2017). Application of gene expression programming to predict daily dew point temperature. *Applied Thermal Engineering*, 112: 1097–1107.

Mentaschi L, Besio G, Cassola F, Mazzino A (2013). Problems in RMSE-based wave model validations. *Ocean Modelling*, 72: 53–58.

Meroney RN (1988). Wind-tunnel modeling of the flow about bluff bodies. *Journal of Wind Engineering and Industrial Aerodynamics*, 29: 203–223.

Mohanta A, Patra K, Sahoo B (2018). Anticipate manning's coefficient in meandering compound channels. *Hydrology*, 5(3): 47.

Muehleisen RT, Patrizi S (2013). A new parametric equation for the wind pressure coefficient for low-rise buildings. *Energy and Buildings*, 57: 245–249.

Najafzadeh M, Azamathulla HM (2015). Neuro-fuzzy GMDH to predict the scour pile groups due to waves. *Journal of Computing in Civil Engineering*, 29(5): 04014068.

Najafzadeh M, Lim SY (2015). Application of improved neuro-fuzzy GMDH to predict scour depth at sluice Gates. *Earth Science Informatics*, 8: 187–196.

Ohkuma T, Marukawa H, Niihori Y, Kato N (1991). Full-scale measurement of wind pressures and response accelerations of a high-rise building. *Journal of Wind Engineering and Industrial Aerodynamics*, 38: 185–196.

Pradhan A, Khatua KK (2018). Gene expression programming to predict Manning's n in meandering flows. *Canadian Journal of Civil Engineering*, 45: 304–313.

Savic DA, Walters GA, Davidson JW (1999). A genetic programming approach to rainfall-runoff modelling. *Water Resources Management*, 13: 219–231.

Stathopoulos T, Zhou YS (1993). Numerical simulation of wind-induced pressures on buildings of various geometries. *Journal of Wind Engineering and Industrial Aerodynamics*, 46–47: 419–430.

Suresh Kumar K, Irwin PA, Davies A (2006). Design of tall building for wind: wind tunnel vs. codes/standards. *Third* In: Proceedings of National Conference on Wind Engineering, Calcutta, India, pp. 318–325.

Swami MV, Chandra S (1987). Procedures for calculating natural ventilation airflow rates in buildings. ASHRAE Final Report FSEC-CR-163-86, ASHRAE Research Project.

Swami MV, Chandra S (1988). Correlations for pressure distribution on buildings and calculation of natural-ventilation airflow. *ASHRAE Transactions*, 94(1): 243–266.

Walker IS, Wilson DJ (1993). Evaluating models for superposition of wind and stack effect in air infiltration. *Building and Environment*, 28: 201–210.

Walton GN (1982). Airflow and multiroom thermal analysis. *ASHRAE Transactions*, 88(2): 78–91.

Wang S, Fu Z, Chen H, Nie Y, Wang K (2016). Modeling daily reference ET in the Karst area of northwest Guangxi (China) using gene expression programming (GEP) and artificial neural network (ANN). *Theoretical and Applied Climatology*, 126: 493–504.

Whigham PA, Crapper PF (1999). Time series modelling using genetic programming: An application to rainfall-runoff models. In: Spector L, Langdon WB, O'Reilly U-M, Angeline PJ (eds), Advances in Genetic Programming, Vol 3. Cambridge, MA, USA: MIT Press. pp. 89–104.

Whigham PA, Crapper PF (2001). Modelling rainfall-runoff using genetic programming. *Mathematical and Computer Modelling*, 33: 707–721.

Yi J, Li QS (2015). Wind tunnel and full-scale study of wind effects on a super-tall building. *Journal of Fluids and Structures*, 58: 236–253.

Zhou Y, Stathopoulos T (1997). A new technique for the numerical simulation of wind flow around buildings. *Journal of Wind Engineering and Industrial Aerodynamics*, 72: 137–147.